Elsevier has created a Monkeypox Information Center in response to the declared public health emergency of international concern, with free information in English on the monkeypox virus. The Monkeypox Information Center is hosted on Elsevier Connect, the company's public news and information website.

Elsevier hereby grants permission to make all its monkeypox related research that is available on the Monkeypox Information Center - including this research content - immediately available in publicly funded repositories, with rights for unrestricted research re-use and analyses in any form or by any means with acknowledgement of the original source. These permissions are granted for free by Elsevier for as long as the Monkeypox Information Center remains active.

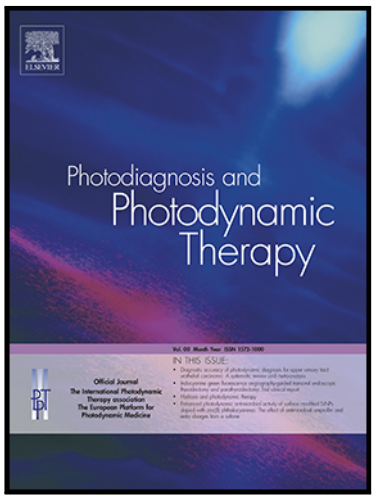

Virtual screening and computational simulation analysis of antimicrobial photodynamic therapy using propolis-benzofuran A to control of Monkeypox

Maryam Pourhajibagher , Abbas Bahador

PII: S1572-1000(22)00494-X
DOI: https://doi.org/10.1016/j.pdpdt.2022.103208
Reference: PDPDT 103208

To appear in: *Photodiagnosis and Photodynamic Therapy*

Received date: 10 October 2022
Revised date: 5 November 2022
Accepted date: 18 November 2022

Please cite this article as: Maryam Pourhajibagher , Abbas Bahador , Virtual screening and computational simulation analysis of antimicrobial photodynamic therapy using propolis-benzofuran A to control of Monkeypox, *Photodiagnosis and Photodynamic Therapy* (2022), doi: https://doi.org/10.1016/j.pdpdt.2022.103208

Virtual screening and computational simulation analysis of antimicrobial photodynamic therapy using propolis-benzofuran A to control of Monkeypox

Maryam Pourhajibagher [1], Abbas Bahador [2,3*]

[1] Dental Research Center, Dentistry Research Institute, Tehran University of Medical Sciences, Tehran, Iran.
[2] Department of Microbiology, School of Medicine, Tehran University of Medical Sciences, Tehran, Iran.
[3] Fellowship in Clinical Laboratory Sciences, BioHealth Lab, Tehran, Iran.

Corresponding author:
*** Dr. Abbas Bahador**
Professor in Medical Microbiology, Department of Microbiology, Tehran University of Medical Sciences, Tehran, Iran.
E-mail: abahador@sina.tums.ac.ir
Telefax: (+98) 21-88955810.

Highlights:

- Propolis-benzofuran A obeyed all the criteria of Lipinski's rule of five and exhibited drug-likeness.
- The molecular docking exhibited a good binding affinity (-7.84 kcal/mol) between Monkeypox virus A48R protein and propolis-benzofuran A ligand.
- Propolis-benzofuran A-mediated aPDT can be proposed as an adjuvant treatment against Monkeypox virus.

Abstract

Background: Monkeypox is a viral zoonotic disease and there are no available treatments that specifically target the monkeypox virus. Antimicrobial photodynamic therapy (aPDT) is a non-invasive approach that has been introduced as a targeted adjuvant treatment against various microbial infections. In this study, we used a computational strategy to investigate the potential of aPDT using propolis-benzofuran A against the Monkeypox virus.

Methods: In this *in silico* study, the evaluation of drug-likeness, molecular properties, and bioactivity of propolis-benzofuran A was carried out using SwissADME. Pro-Tox II and OSIRIS

servers were used to identify the organ toxicities and toxicological endpoints of propolis-benzofuran A. Molecular docking approach was employed to screen the potential binding modes of propolis-benzofuran A ligand with the Monkeypox virus A48R protein (PDB ID: 2V54).

Results: The results of the computational investigation revealed that propolis-benzofuran A obeyed all the criteria of Lipinski's rule of five and exhibited drug-likeness. The photosensitizing agent tested was categorized as toxicity class-5 and was found to be non-hepatotoxic, non-carcinogenic, non-mutagenic, and non-cytotoxic. The docking studies employing a predicted three-dimensional model of Monkeypox virus A48R protein with propolis-benzofuran A ligand exhibited good binding affinity (-7.84 kcal/mol).

Discussion: The computational simulation revealed that propolis-benzofuran A had a strong binding affinity with the Monkeypox virus A48R protein. Hence, aPDT based on this natural photosensitizer can be proposed as an adjuvant treatment against the Monkeypox virus.

Keywords: Antimicrobial photodynamic therapy, *In silico*, Monkeypox, Propolis

1 Introduction

Monkeypox is a zoonotic contagious disease with multiple reservoirs that the World Health Organization (WHO) announced its re-emergence in July 2022 [1]. Monkeypox virus belongs to the Orthopoxvirus genus of the Poxviridae family, which encompasses human-associated pathogens such as the variola virus, the causative agent of smallpox, the cowpox virus, the camelpox virus, as well as the vaccinia virus [2]. In the current outbreak, either the disease appearing mildly or asymptomatically, and sustained human-to-human transmission seen in this outbreak has not been previously observed [3]. According to Prichard et al., A48R, A50R, D13L protein trimer complex, F13L, and I7L have been proposed as useful interventions for poxvirus targets by other studies and reviews. Among them, A48R has been identified to be a good potential drug target [4]. A48R as a thymidylate kinase is a novel target and is currently not targeted by any known drugs. A48R phosphorylates thymidine monophosphate (TMP), also known as thymidylic acid, to its diphosphate (DP) and also to phosphorylate 50 halogenated deoxyuridine monophosphate (dUMP) analogs [4].

One to three days after the onset of flu-like prodromal symptoms (e.g., fever, malaise, chills, headache, weakness, lymphadenopathy), rash and lesions appear on the face and extremities, and oral mucous membranes, genitalia, conjunctivae, and cornea are affected [1]. Due to the lack of an effective treatment that eliminates the virus, there is an urgent need to develop an appropriate strategy to control the pathogenicity of the Monkeypox virus. One of the approaches used to control the Monkeypox virus can be antimicrobial photodynamic therapy (aPDT). According to the literature, there are several *in vitro* studies and clinical trials of systemic and topical aPDT as a treatment approach and adjuvant therapy for various viral infections [6-10].

aPDT involves a synergic association of a non-toxic dye called a photosensitizer, visible light with a specific wavelength, and oxygen, which can produce reactive oxygen species (ROS), causing

irreversible damage to the lipid or protein-membrane structures of the viral envelope, even nucleic acid, without damaging the surrounding tissue [11-13]. Natural products have received a lot of attention among photosensitizers made from various chemical compounds commonly employed in aPDT.

Propolis is one of the honeybee's products that has a wide range of medical effects [14]. Many studies documented various biological properties of propolis such as antimicrobial, antioxidant, antitumor, and anti-inflammatory [15-18]. Propolis benzofuran A and B are two main important chemical compounds in the propolis that their biological activity is a topic of main interest for organic chemists and biologists [14]. However, the association of aPDT with propolis has not been widely studied.

It is important to identify the viral-relevant molecular targets with appropriate sensitivity to aPDT. As the previous studies revealed the computational analysis enhances our knowledge of the target site for increasing the efficiency of targeted aPDT [19-22]. In this study, we used a number of biological databases and bioinformatics tools to predict the potential of aPDT using propolis-benzofuran A to control of Monkeypox virus.

2 Methods

2.1. Preparation of target

Monkeypox virus A48R protein was used as the selected target protein for this study. Complete sequences of A48R were downloaded from the NCBI Nucleotide database (GenBank accession: AGR38144.1). The Protein Basic Local Alignment Search Tool (BLAST-P) was used for the identification of the most similar template in the PDB database, and then the template with the best score was selected for model generation.

2.2. Validation of homology model

The physicochemical properties and functional characterization of predicted protein such as protein molecular weight, extinction coefficient, isoelectric point, instability index, aliphatic index, and grand average of hydropathicities were predicted using the ProtParam ExPASy tool. The helices, sheets, and turns of amino acid sequences related to the secondary structure of the Monkeypox virus A48R protein were predicted by SOPMA-based secondary structure prediction. The crystal structure of thymidylate kinase (PDB ID: 2V54) was used as a template for the Monkeypox virus A48R protein. The three-dimensional structure of the target protein was modeled using the Swiss-MODEL. The authenticity of the model was evaluated by Ramachandran scores using the PROCHECK server, and the quality of the model structure was validated using ERRAT, Verify_3D, and ProSA-web servers.

2.3. Ligand’s retrieval and preparation

The three-dimensional structure of propolis-benzofuran A, as a natural photosensitizer, was achieved from PubChem (www.pubchem.com) in .sdf format.

2.4. *In silico* pharmacokinetics (ADME) and toxicological properties

According to the previous studies [22], *in silico* prediction of ADME via the SwissADME and admetSAR programs was conducted to confirm whether the physicochemical properties of propolis-benzofuran A as the ligand follows Lipinski's rule of five or not. Lipinski's rule of five displays that the candidate should obey the five-parameter rule, which states that hydrogen-bond donors (HBDs) should be less than 5, hydrogen-bond acceptors (HBAs) should be less than 10, the molecular mass should be less than 500 Da, lipophilicity (expressed as Log P) should not be less than 5, and total polar surface area (TPSA) should not be greater than 140Å [244]. The organ toxicities and toxicological endpoints of propolis-benzofuran A were predicted using Pro-Tox II and OSIRIS servers.

2.5. Structure-based pharmacological activity and metabolism prediction

The biological activity of propolis-benzofuran A molecule concerning the probability of activity (Pa) and inactivity (Pi) was predicted using the PASS server as follows:
Pa>0.7: The compound is very likely to exhibit the activity,
0.7>Pa>0.5: The compound is likely to exhibit the activity,
Pa<0.5: The compound is less likely to exhibit activity.

2.6. Molecular docking analysis

Molecular docking analysis was performed to check the binding sites and interactions that occur between the candidates and the proteins. Herein, the potential binding modes of ligand (propolis-benzofuran A) to receptor (Monkeypox virus A48R protein) in its respective PDB structure (ID: 2V54) was assessed via the SwissDock server. A protein-ligand complex with the lowest binding energy (kcal/mol) was then selected as the most favored confirmation to explain the interaction.

3 Results

3.1. Sequence retrieval analysis

As previously mentioned, thymidylate kinase (PDB ID: 2V54) was utilized as a template model for the prediction of the Monkeypox virus A48R protein structure. Basic information obtained from 2V54 showed that it had 204 amino acids with a molecular weight of 23377.77 Da. The amino acid compositions of 2V54 were as follows: Alanine (Ala) 4.9%; Arginine (Arg) 2.9%; Asparagine (Asn) 4.4%; Aspartic acid (Asp) 4.4%; Cysteine (Cys) 1.0%; Glutamine (Gln) 4.9%; Glutamic acid (Glu) 9.8%; Glycine (Gly) 6.3%; Histidine (His) 1.5%; Isoleucine (Ile) 9.8%; Leucine (Leu) 7.3%; Lysine (Lys) 7.8%; Methionine (Met) 3.4%; Phenylalanine (Phe) 4.4%; Proline (Pro) 2.4%; Serine (Ser) 6.8%; Threonine (Thr) 6.3%; Tryptophan (Trp) 1.5%; Tyrosine (Tyr) 3.9%; and Valine (Val) 6.3%. Moreover, the number of positively (Arg + Lys) and negatively (Asp + Glu) charged residues of 2V54 were 22 and 29, respectively. The results of the ProtParam ExPASy tool showed that the extinction coefficient of 2V54 in water at 280 nm was found to be 28545 M^{-1} cm^{-1}. Also, the isoelectric point, instability index, aliphatic index, and grand average of hydropathicities were computed to be 5.11, 48.18, 89.85, and -0.246, respectively.

3.2. Model evaluation

The secondary structure of protein chains was analyzed by SOPMA which predicted the alpha helix, random coil, extended strand, and beta-turn. In the designed secondary structure of 2V54, alpha helices showed 46.34%. It is followed by random coils (30.24%), extended strands (15.61%), and beta-turn (7.80%), respectively. According to the results, the 2V54 revealed the predominant nature of helices.

The predicted three-dimensional structure for the Monkeypox virus A48R protein is presented in Figure 1. As seen in Figure 1, 2V54 consists of 2 chains A and B, and 3 ligands named TYD (Thymidine-5'-diphosphate), POP (Pyrophosphate 2-), and magnesium ion (Mg^{2+}). Some properties of chains and ligands are listed in Table 1.

Multiple methods were employed for the validation of the three-dimensional models. The modeled tertiary structure was validated by PROCHECK's Ramachandran plot analysis, Verify_3D, ERRAT, and ProSA-web servers. The Ramachandran plot analysis (Fig. 2a) displayed that the number of residues in the most favored region was 88.8%, which is an indicator of a valid model. Also, 10.4% of residues were in additional allowed regions. An overall quality factor of 94.615 by ERRAT verified the model as good quality (Fig. 2b). Quality assessment of the homology-predicted structure is made by the ProSA-web algorithm, according to which the final structure obtained a Z-score of -6.1, nested within other proteins of similar size (Fig. 2c). VERIFY_3D result showed that 86.49% of residues had averaged 3D-1D score >= 0.2 and at least 80% of the amino acids had scored >= 0.2 in the 3D/1D profile (Fig. 2d). Hence, the findings indicate that the modeled structure of Monkeypox virus A48R protein is reasonable and reliable as a target for propolis-benzofuran A.

3.3. Drug-likeness prediction

The drug-likeliness of propolis-benzofuran A was performed using Lipinski's rule of five. As shown in Table 2, the photosensitizing agent screened for the study was found to obey all the criteria of Lipinski's rule. According to this rule, the molecular weight was 452.45 g/mol (acceptable range: < 500), the number of hydrogen bond donors was 2 (acceptable range: ≤ 5), the number of hydrogen bond acceptors was 8 (acceptable range: ≤ 10), Log P was 3.96 (acceptable range: < 5), and TPSA was 115.43 Å² (acceptable range: < 140). The computational study suggests the molecules can act as excellent orally active drugs.

3.4. ADME analysis

The parameters of SwissADME prediction showed that propolis-benzofuran A had high gastrointestinal (GI) absorption without blood-brain barrier (BBB) permeation (Table 3). Moreover, propolis-benzofuran A inhibited cytochromes CYP2C9 and CYP3A4, as well as the substrate of permeability glycoprotein (P-gp). Also, the skin permeation value (log Kp) of the photosensitizing compound was found to be in the range of -4.5 to - 7.2 cm/s. This clearly shows the low skin permeability of propolis-benzofuran A.

3.5. Toxicity prediction

Propolis-benzofuran A was computed by Pro-Tox II and OSIRIS servers to assess its toxicity such as hepatotoxicity, carcinogenicity, immunotoxicity, mutagenicity, and cytotoxicity. The findings of toxicological prediction indicated that propolis-benzofuran A is non-hepatotoxic, non-carcinogenic, immunogenic and non-cytotoxic suggesting this this photosensitizing compound as may be good candidates in this investigation (Table 4).

3.6. Pharmacological activity and metabolism prediction

The results of the pharmacological activity prediction of propolis-benzofuran A are presented in Table 5. It was found that there were three pharmacological activities with a Pa score greater than 0.7. In addition, half of the metabolic activity of this photosensitizer compound is at the prediction threshold of 0.7>Pa>0.5.

3.7. Molecular docking analysis

Asn65, Asp92, Lys105, Ala107, Leu111, Tyr143, Ala190, and Thr195 were the important residues and the active binding regions of the Monkeypox virus A48R protein that were predominantly engaged in ligand-protein interaction (Fig. 3). According to the *in silico* molecular docking analysis, the propolis-benzofuran A showed the binding affinity value of -7.84 kcal/mol in relation to the A48R protein.

4 Discussion

As WHO reported, the fatality ratio of monkeypox is around 3 to 6% [23]. Although the smallpox vaccine may prevent monkeypox in some people, there is no appropriate treatment protocol for monkeypox [24]. In recent years, new treatment methods have been proposed to deal with viral infections. aPDT has advantages that make its use more efficient than other methods, including a broad spectrum of action, the efficient inactivation of antibiotic-resistant microorganisms, the lack of selection of photo-resistant microbial cells, and the minimal mutagenic potential [25].

The effect of aPDT as adjunct therapy on viral infections such as Middle East Respiratory Syndrome (MERS), influenza, and coronavirus was previously reported [26-29]. Jin et al. [26] showed that aPDT with 1, 2, and 4 μM of methylene blue with light irradiation at a wavelength of 630 nm for 2 min could be effective against severe acute respiratory syndrome coronavirus 2 (SARS-CoV-2) in plasma without any side effects. In other studies, Eickmann et al. [27,28] displayed methylene blue plus visible light at the light doses as low as 30 J/cm^2 reduced SARS-CoV and MERS-CoV more than 3.1 and 3.3 log10 TCID50/mL in plasma, respectively. Also, the ability of aPDT as a treatment approach and adjuvant therapy using curcumin-poly (lactic-co-glycolic acid) nanoparticles (Cur@PLGA-NPs) to inactivate COVID-19 in plasma was investigated by Pourhajibagher et al. [29]. Their findings showed that aPDT using 10% wt. Cur@PLGA-NPs and a blue laser at an energy density of 522.8 J/cm^2 exhibited in vitro anti-COVID-19 activities in the treated plasma containing SARS-COV-2 without Vero cell apoptosis

and any adverse effects on plasma quality in aPDT-exposed plasma. Hence, the use of aPDT can be an adjunct approach against the Monkeypox virus that deserves to be explored.

The specific binding of photosensitizer to the target site causes effective phototoxicity against microorganisms and site-specific accumulation of the photosensitizer in microorganisms after systemic administration, which is correlated with microorganisms' eradication following light irradiation. The disparate effectiveness of aPDT can be due to variations in the target sites of the photosensitizer. On the other hand, it is unknown which structure of the microorganism can bind to the photosensitizer. In this study, we introduced the A48R as a target site in the Monkeypox virus using molecular modeling and simulation analysis through several data banks.

Various physicochemical properties of 2V54 as a template for the Monkeypox virus A48R protein were assessed by the ProtParam ExPASy tool, which indicated that the predicted protein would be stable (index value of 48.18); the isoelectric point was found to be 5.11; and the aliphatic index of the protein was estimated at 89.85, which is an indication of a thermostable protein. In addition, the GRAVY value was estimated to be -0.246, which indicates that the protein may interact with water.

After the prediction of a three-dimensional structure, the stereochemical quality of the predicted model structure, the compatibility of the atomic model (3D) of the predicted protein with its amino acid sequence (1D), non-bonded atomic interactions, and the refinement and validation of the predicted protein model were assessed using PROCHECK, Verify_3D, ERRAT, and ProSA-web servers, respectively [30-34]. As per the results, the predicted model is of good quality.

In the present study, the SwissADME server was used to analyze various ADME descriptors like, physiochemical properties, pharmacokinetics, solubility, lipophilicity, and drug-likeness based on violation of Lipinski's. The *in silico* ADME prediction of propolis-benzofuran A established drug-likeness as evidenced by no violation to its Lipinski's rule of five and the bioavailability score of 0.55. Moreover, the drug metabolism is regulated by a range of cytochromes (CYP), in which CYP1A2, CYP2C9, CYP2C19, CYP2D6, and CYP3A4 are vital for the biotransformation of drug molecules [35]. According to the results, propolis-benzofuran A can inhibit CYP2C9 and CYP3A4. To investigate the *in silico* toxicity parameters, Pro-Tox II and OSIRIS were used. The predicted LD50 (mg/kg) for propolis-benzofuran A was 2160; hence was categorized as toxicity class-5, indicating that the propolis-benzofuran A is not harmful if swallowed (LD50>2000). Further, propolis-benzofuran A was found to be non-hepatotoxic, non-carcinogenic, non-mutagenic, and non-cytotoxic.

To achieve the topical properties of propolis, active compounds of propolis should penetrate the epidermis and into the dermis. This is mainly important if topical skin products containing propolis are considered for use as a photosensitizer in aPDT. It has been found that the biologically active components of propolis are mainly phenolic compounds including cinnamic acid and benzoic acid derivatives [36,37]. Cinnamic acid derivatives including coumaric acid, caffeic acid, and ferulic acid, induced a more significant increase in membrane permeation than benzoic acid derivatives such as vanillic acid and this effect was attributed to differences in structural features of these phenolic acids [38].

The parameters of ADME prediction in the current study showed that the skin permeation value (log Kp) of the propolis-benzofuran A was found to be in the range of -4.5 to -7.2 cm/s, which shows the low skin permeability of propolis-benzofuran A. However, Ramanauskiene et al. [https://doi.org/10.2478/acph-2021-0044], in a study on full-thickness undamaged human skin, showed that the phenolic compounds of propolis can penetrate the epidermis and dermis from all formulations of ointment, cream, and emulsion. However, the largest quantity of active compounds is absorbed from ointment than the emulsion system. This could have been due to fatty acids contained in beeswax and sunflower oil, which are described previously as effective enhancers of penetration [39].

It has been revealed that the quantity of penetrated coumaric and ferulic acids found in the epidermis was significantly greater than in the dermis. While the quantities of penetrated vanillic acid found in the dermis area were significantly higher than those found in the epidermis. Caffeic acid does not penetrate the epidermis or the dermis. In a recent study, Oliveira et al. [38] found that coumaric acid, caffeic acid, and ferulic acid exhibit antimicrobial synergism with light, however, coumaric acid did not present antimicrobial synergism with light.

In cutaneous monkeypox lesions, the basal layer seems to be the site of the initial infection. Immunohistochemical staining of cutaneous biopsies revealed that viral antigens are found within keratinocytes and a few Langerhans cells of the epidermis. Electron microscopy also showed abundant virions at various stages of assembly, immature and mature orthopoxvirus particles, within the keratinocyte cytoplasm in the epidermis [40].

Overall, since cutaneous monkeypox mainly affects the epidermis and to a lesser extent the dermis and active compounds of propolis can penetrate the epidermis and dermis and be activated by the light there, it seems that nano-propolis and light have a synergistic effect in removing the monkeypox viruses. This hypothesis, which is based on the available evidence should be evaluated by in vitro and clinical trial studies toward efforts to manage and also reduce the severity of monkeypox infections using targeted nano-propolis mediated aPDT.

It has been found from Monte Carlo simulations that maximum penetration depths using the Intense pulsed light system were found to be 0.5 mm and 1 mm for light with 300 nm and 400 nm wavelength, respectively using the 1% criterion [41]. Since the diameter of the epidermis is about 70 µm and the highest virus load is found in this area [40], and active compounds of propolis also penetrate in this depth, therefore it is possible to activate the active compounds of propolis by light in the epidermis and inactivate the monkeypox viruses in this area. To inactivate monkeypox viruses in the deeper area of the skin, i.e. dermis, it is necessary to use increasing spot size and longer wavelengths of light. Studies have shown that an increase in penetration depth can be achieved using increasing spot size employed by the device and longer wavelengths of light.

With an increasing spot size, of at least 10 mm in width, there is a decrease in the amount of lateral scattering; this results in higher penetration light [41]. As a result, a device with at least 10 mm in spot size can be applied to achieve a greater penetration depth for the treatment of cutaneous monkeypox lesions. Another way to increase the penetration depth of light is to use light with a higher wavelength [41]. It is clear that when using light with higher wavelengths, photosensitizers

that absorb light at higher wavelengths should be used. It has shown that by changing the structure of photosensitizers, they may be activated by lights with higher wavelengths.
It has been shown that the complexation of rutin with metal ions in aluminum chloride and thorium solution can lead to a shift in its absorption spectrum from the UVA range (355 nm) to the visible spectrum (425 nm) [42,43]. This change makes greater penetration of light and activation of rutin in the deeper area of tissue in the clinical setting. In this regard, recently Halevas et al. [44], introduce the curcumin-gallium complex as a novel photosensitizer in PDT against breast cancer cells with a significant red-shift in the absorption spectrum and comparable ROS generation compared to plain curcumin, which they are highly desirable properties for a photosensitizer. Considering all these aspects, it may be possible to obtain a photosensitizer with the ability to be activated at higher wavelengths of light by changing the structure of propolis, which is more effective in the treatment of monkeypox infections.
Molecular docking is an approach to mimic intermolecular binding modes and the interaction of key residues with the ligand. In this study, a molecular docking experiment provides the docking model of interactions between the Monkeypox virus A48R protein and propolis-benzofuran A. The findings revealed that propolis-benzofuran A and A48R had a strong bond with the lowest binding energy value of -6.2 kcal/mol. According to the results of this *in silico* study, it can be concluded that aPDT using propolis-benzofuran A can target purposefully Monkeypox virus A48R protein. Eventually, aPDT at a wavelength in the region between 250 and 400 nm [45] can collapse the structure of the viral cells through the generation of ROS and prevent the attachment of viruses to the host cell surface.
This *in silico* study might be a valuable contribution to the field of bioinformatics research in in the control of the Monkeypox virus. In addition, it may help other researchers to get an idea about the protein structure and its physicochemical properties to perform extensive examinations on the design and manufacture of drugs and/or vaccines against the Monkeypox disease, as well as define the therapeutic protocols for patients with Monkeypox who present rash and lesions on their face and extremities.

5 Conclusion

In summary, the computational simulation analysis indicated Monkeypox virus A48R protein is a stable protein. According to the biological databases and bioinformatics tools, propolis benzofuran A not only had acceptable pharmacokinetic and pharmacodynamic properties but also interacted with A48R with high affinity. Hence, targeted aPDT using propolis-benzofuran A can be considered a potential treatment to control Monkeypox.

Declaration of competing interest

The authors declare that there are no conflicts of interest regarding the publication of this paper.

Acknowledgments

Not applicable.

Funding
Not applicable.

References

1. Schnierle BS. Monkeypox Goes North: Ongoing Worldwide Monkeypox Infections in Humans. Viruses. 2022 Aug 25;14(9):1-7.

2. Alkhalil A, Strand S, Mucker E, Huggins JW, Jahrling PB, Ibrahim SM. Inhibition of Monkeypox virus replication by RNA interference. Virology Journal. 2009 Dec;6(1):1-0.

3. Riopelle JC, Munster VJ, Port JR. Atypical and unique transmission of monkeypox virus during the 2022 outbreak: an overview of the current state of knowledge. Viruses. 2022 Sep 11;14(9):2012.

4. Prichard MN, Kern ER. Orthopoxvirus targets for the development of new antiviral agents. Antiviral research. 2012 May 1;94(2):111-25.

5. Lam HY, Guan JS, Mu Y. In silico repurposed drugs against monkeypox virus. Molecules. 2022 Aug 18;27(16):5277.

6. Ramires MC, Mattia MB, Tateno RY, Palma LF, Campos L. A combination of phototherapy modalities for extensive lip lesions in a patient with SARS-CoV-2 infection. Photodiagnosis and Photodynamic Therapy. 2021 Mar 1;33:102196.

7. Teitelbaum S, Azevedo LH, Bernaola-Paredes WE. Antimicrobial photodynamic therapy used as first choice to treat herpes zoster virus infection in younger patient: A case report. Photobiomodulation, Photomedicine, and Laser Surgery. 2020 Apr 1;38(4):232-6.

8. Vellappally S, Mahmoud MH, Alaqeel SM, Alotaibi RN, Almansour H, Alageel O, et al. Efficacy of antimicrobial photodynamic therapy versus antiviral therapy in the treatment of herpetic gingivostomatitis among children: a randomized controlled clinical trial. Photodiagnosis and Photodynamic Therapy. 2022 Apr 30:102895.

9. Khorsandi K, Fekrazad S, Vahdatinia F, Farmany A, Fekrazad R. Nano antiviral photodynamic therapy: a probable biophysicochemical management modality in SARS-CoV-2. Expert Opinion on Drug Delivery. 2021 Feb 1;18(2):265-72.

10. Raffaele RM, Baldo ME, Santana GU, Siqueira JM, Palma LF, Campos L. Phototherapies for erythema multiforme secondary to viral infections: A case report of a child. Photodiagnosis and Photodynamic Therapy. 2022 Dec 1;40:103094.

11. Namvar MA, Vahedi M, Abdolsamadi HR, Mirzaei A, Mohammadi Y, Jalilian FA. Effect of photodynamic therapy by 810 and 940 nm diode laser on Herpes Simplex Virus 1: An in vitro study. Photodiagnosis and Photodynamic Therapy. 2019 Mar 1;25:87-91.

12. Cieplik F, Deng D, Crielaard W, Buchalla W, Hellwig E, Al-Ahmad A, Maisch T. Antimicrobial photodynamic therapy–what we know and what we don't. Critical Reviews in Microbiology. 2018 Sep 3;44(5):571-89.

13. Vatansever F, de Melo WC, Avci P, Vecchio D, Sadasivam M, Gupta A, et al. Antimicrobial strategies centered around reactive oxygen species–bactericidal antibiotics, photodynamic therapy, and beyond. FEMS microbiology reviews. 2013 Nov 1;37(6):955-89.

14. Rouhani M. A detailed computational investigation on the structural and spectroscopic properties of propolisbenzofuran B. Heliyon. 2019 Oct 1;5(10):e02518.

15. Wang K, Ping S, Huang S, Hu L, Xuan H, Zhang C, Hu F. Molecular mechanisms underlying the in vitro anti-inflammatory effects of a flavonoid-rich ethanol extract from Chinese propolis (poplar type). Evidence-Based Complementary and Alternative Medicine. 2013 Jan 1;2013.

16. Xuan H, Zhao J, Miao J, Li Y, Chu Y, Hu F. Effect of Brazilian propolis on human umbilical vein endothelial cell apoptosis. Food and chemical toxicology. 2011 Jan 1;49(1):78-85.

17. Xuan H, Zhu R, Li Y, Hu F. Inhibitory effect of chinese propolis on phosphatidylcholine-specific phospholipase C activity in vascular endothelial cells. Evidence-Based Complementary and Alternative Medicine. 2010;2011.

18. Bankova VS, de Castro SL, Marcucci MC. Propolis: recent advances in chemistry and plant origin. Apidologie. 2000 Jan 1;31(1):3-15.

19. Pourhajibagher M, Bahador A. Evaluation of the crystal structure of a fimbrillin (FimA) from Porphyromonas gingivalis as a therapeutic target for photo-activated disinfection with toluidine blue O. Photodiagnosis Photodyn Ther. 2017; 17: 98-102.

20. Pourhajibagher M, Bahador A. Outer membrane protein 100 of Aggregatibacter actinomycetemcomitans act as a biopharmaceutical target for photodynamic therapy: An in silico analysis. Photodiagnosis Photodyn Ther. 2016; 16: 154-160.

21. Pourhajibagher M, Bahador A. Designing and in silico analysis of PorB Protein from Chlamydia Trachomatis for developing a vaccine candidate. Drug Res (Stuttg). 2016; 66: 479-483.

22. Pourhajibagher M, Bahador A. Molecular docking study of potential antimicrobial photodynamic therapy as a potent inhibitor of SARS-CoV-2 main protease: An in silico insight. Infectious Disorders Drug Targets. 2022 [Epub head of print].

23. Available online: https://www.who.int/news-room/fact-sheets/detail/monkeypox, (accessed on 19 May 2022).

24. Available online: https://www.cdc.gov/poxvirus/monkeypox/about/faq.html, (accessed on 28 September 2022).

25. Celiešiūtė-Germanienė R, Šimonis P, Stirkė A. Antimicrobial photodynamic therapy (aPDT) for biofilm treatments. Possible synergy between aPDT and pulsed electric fields. Virulence. 2021;12(1):2247.

26. Jin C, Yu B, Zhang J, Wu H, Zhou X, Yao H, et al. RETRACTED ARTICLE: Methylene blue photochemical treatment as a reliable SARS-CoV-2 plasma virus inactivation method for blood safety and convalescent plasma therapy for COVID-19. BMC Infectious Diseases. 2021 Dec;21(1):1-8.

27. Eickmann M, Gravemann U, Handke W, Tolksdorf F, Reichenberg S, Müller TH, et al. Inactivation of three emerging viruses–severe acute respiratory syndrome coronavirus, Crimean–Congo haemorrhagic fever virus and Nipah virus–in platelet concentrates by ultraviolet C light and in plasma by methylene blue plus visible light. Vox sanguinis. 2020 Apr;115(3):146-51.

28. Eickmann M, Gravemann U, Handke W, Tolksdorf F, Reichenberg S, Müller TH, et al. Inactivation of Ebola virus and Middle East respiratory syndrome coronavirus in platelet concentrates and plasma by ultraviolet C light and methylene blue plus visible light, respectively. Transfusion. 2018 Sep;58(9):2202-7.

29. Pourhajibagher M, Azimi M, Haddadi-Asl V, Ahmadi H, Gholamzad M, Ghorbanpour S, Bahador A. Robust antimicrobial photodynamic therapy with curcumin-poly (lactic-co-glycolic acid) nanoparticles against COVID-19: a preliminary in vitro study in Vero cell line as a model. Photodiagnosis and Photodynamic Therapy. 2021 Jun 1;34:102286.

30. Wiederstein M, Sippl MJ. ProSA-web: interactive web service for the recognition of errors in three-dimensional structures of proteins. Nucleic acids research. 2007 Jul 1;35(suppl_2):W407-10.

31. Morris AL, MacArthur MW, Hutchinson EG, Thornton JM. Stereochemical quality of protein structure coordinates. Proteins: Structure, Function, and Bioinformatics. 1992 Apr;12(4):345-64.

32. Kleywegt GJ, Jones TA. Phi/psi-chology: Ramachandran revisited. Structure. 1996 Dec 15;4(12):1395-400.

33. Eisenberg D, Lüthy R, Bowie JU. [20] VERIFY3D: assessment of protein models with three-dimensional profiles. InMethods in enzymology 1997 Jan 1 (Vol. 277, pp. 396-404). Academic Press.

34. Laskowski RA, MacArthur MW, Moss DS, Thornton JM. PROCHECK: a program to check the stereochemical quality of protein structures. Journal of applied crystallography. 1993 Apr 1;26(2):283-91.

35. Yan Z, Caldwell GW. Metabolism profiling, and cytochrome P450 inhibition & induction in drug discovery. Current topics in medicinal chemistry. 2001 Nov 1;1(5):403-25.

36. Zullkiflee N, Taha H, Usman A. Propolis: Its Role and Efficacy in Human Health and Diseases. Molecules. 2022 Sep 19;27(18):6120.

37. Hochheim S, Guedes A, Faccin-Galhardi L, Rechenchoski DZ, Nozawa C, Linhares RE, et al. Determination of phenolic profile by HPLC–ESI-MS/MS, antioxidant activity, in vitro cytotoxicity and anti-herpetic activity of propolis from the Brazilian native bee Melipona quadrifasciata. Revista Brasileira de Farmacognosia. 2019 Aug 26;29:339-50.

38. de Oliveira EF, Yang X, Basnayake N, Huu CN, Wang L, Tikekar R, et al. Screening of antimicrobial synergism between phenolic acids derivatives and UV-A light radiation. Journal of Photochemistry and Photobiology B: Biology. 2021 Jan 1;214:112081.

39. Mittal A, Sara UV, Ali A, Aqil M. Status of fatty acids as skin penetration enhancers-a review. Current drug delivery. 2009 Jul 1;6(3):274-9.

40. Bayer-Garner IB. Monkeypox virus: histologic, immunohistochemical and electron-microscopic findings. Journal of cutaneous pathology. 2005 Jan;32(1):28-34.

41. Badugu R, Lakowicz JR, Geddes CD. A glucose-sensing contact lens: from bench top to patient. Current opinion in biotechnology. 2005 Feb 1;16(1):100-7.

42. Dev B, Jain BD. Spectrophotometric determination of thorium with rutin (quercetin-3-rutinoside). Journal of the Less Common Metals. 1962 Jun 1;4(3):286-90.

43. Xu H, Li Y, Tang HW, Liu CM, Wu QS. Determination of rutin with UV-Vis spectrophotometric and laser-induced fluorimetric detections using a non-scanning spectrometer. Analytical letters. 2010 Mar 16;43(6):893-904

44. Halevas E, Arvanitidou M, Mavroidi B, Hatzidimitriou AG, Politopoulos K, Alexandratou E, et al. A novel curcumin gallium complex as photosensitizer in photodynamic therapy: Synthesis, structural and physicochemical characterization, photophysical properties and in vitro studies against breast cancer cells. Journal of Molecular Structure. 2021 Sep 15;1240:130485.

45. Ristivojević P, Trifković J, Stanković DM, Radoičić A, Manojlović D, Milojković-Opsenica D. Cyclic voltammetry and UV/Vis spectroscopy in combination with multivariate data analysis for the assessment of authenticity of poplar type propolis. Journal of Apicultural Research. 2017 Oct 20;56(5):559-68.

Figure legends:

Figure 1. The predicted three-dimensional structure for the Monkeypox virus A48R protein.

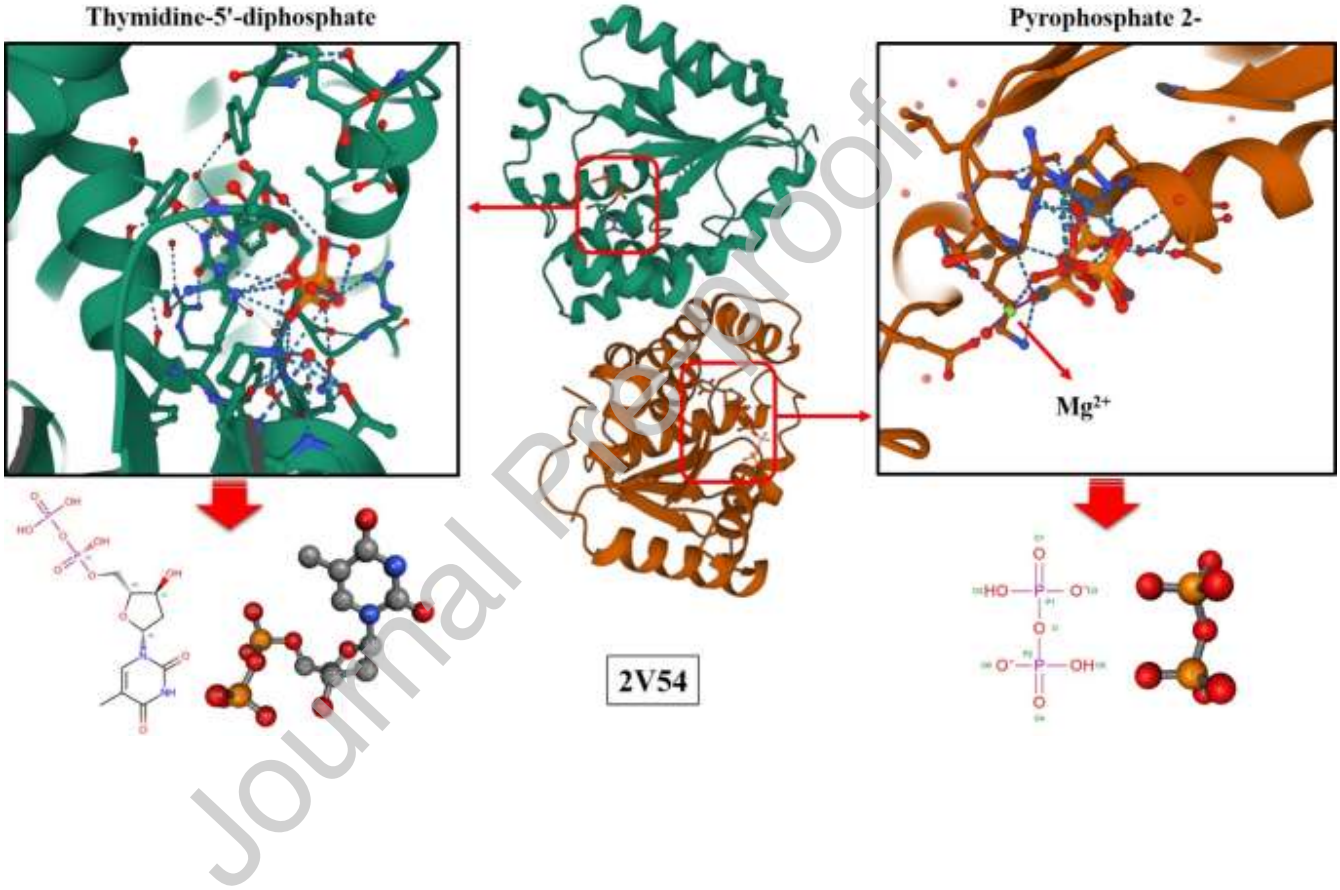

Figure 2. Validation of the Monkeypox virus A48R protein-predicted structure using a. the Ramachandran plot, b. ERRAT, c. Verify_3D, and d. ProSA-web servers.

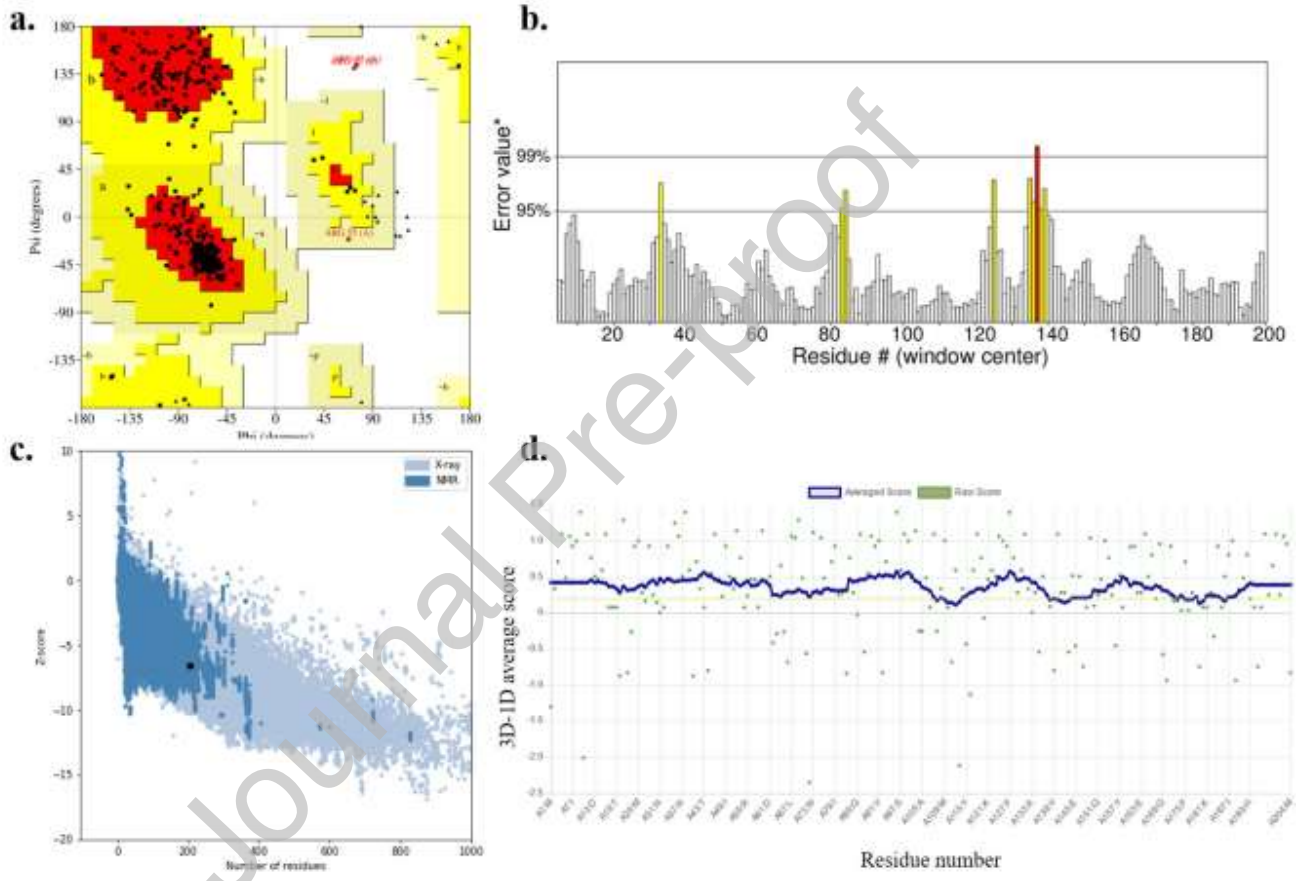

Figure 3. Representation of docked ligand-protein complex: Interaction of propolis-benzofuran A with amino acid residues of the Monkeypox virus A48R protein.

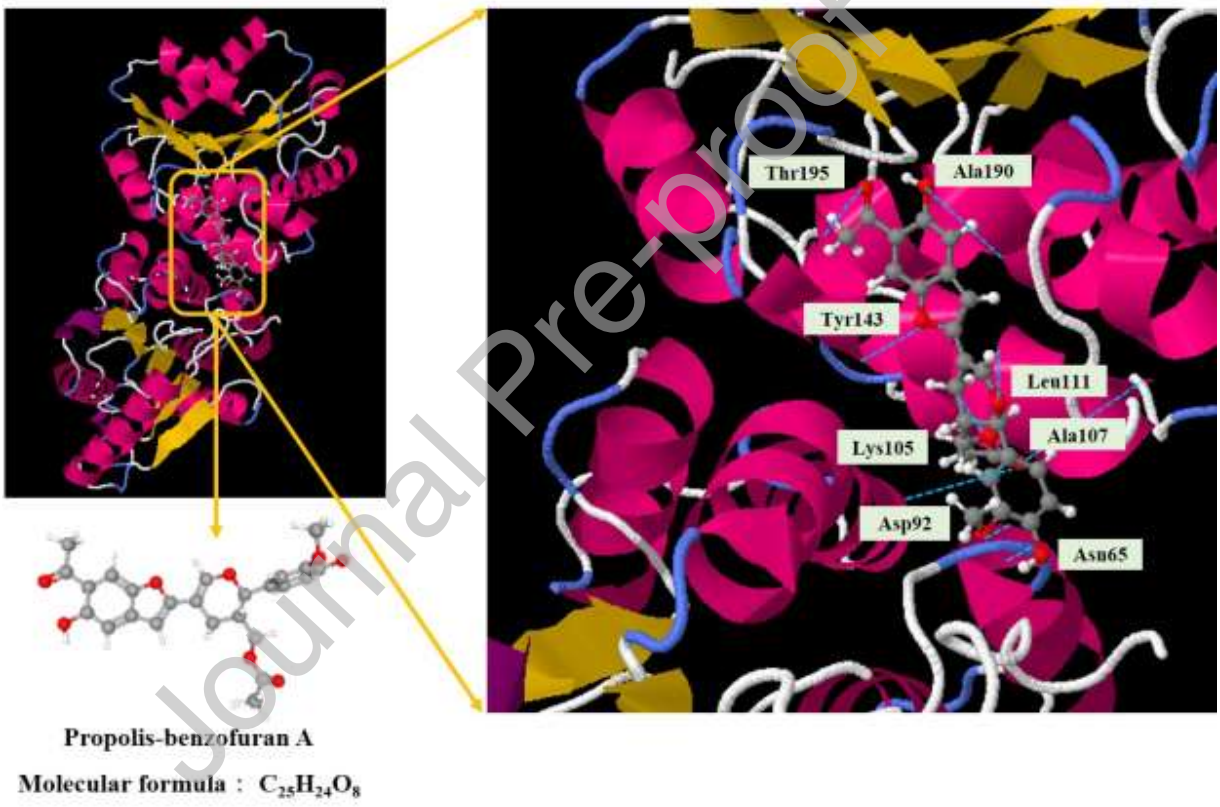

Identifier	Ranking for goodness of fit (%)	Ranking for geometry (%)	Real space R factor	Real space correlation coefficient	RMSZ-bond-length	RMSZ-bond-angle	Outliers of bond length	Outliers of bond angle	Atomic clashes	Stereochemical errors	Model completeness (%)	Average occupancy
TYD A	81	19	0.114	0.967	1.76	1.92	4	10	0	0	100	1
TYD B	58	14	0.177	0.958	1.94	2.11	5	11	0	0	100	0.59
POP	50	0	0.121	0.954	2.36	7.88	2	5	0	0	56	10.56

Table 1. The properties of chains and ligands.

Table 2. Drug likeness property analysis of the natural photosensitizer.

Drug likeness properties	Propolis-benzofuran A
Formula	C25H24O8
Molecular weight	452.45 g/mol
Number of heavy atoms	33
Number of aromatic heavy atoms	15
Fraction Csp3	0.28
Number of rotatable bonds	7
Number of H-bond acceptor	8
Number of H-bond donor	2
Molar refractivity	120.62
LogP	3.27
TPSA	93.06 Å^2

.

Table 3. ADME properties of the natural photosensitizer.

Properties	Propolis-benzofuran A
GI absorption	High
BBB permeant	No
P-gp substrate	Yes
CYP2C19 inhibitor	No
CYP2C9 inhibitor	Yes
CYP2D6 inhibitor	No
CYP3A4 inhibitor	Yes
Skin Permeation Value (log Kp) cm/s	-6.51

Abbreviations: GI, gastro-intestinal; BBB, blood brain barrier; P-gp, P-glycoprotein; CYP, cytochrome-P.

Table 4. Toxicity prediction of the natural photosensitizer.

Properties		Prediction	Probability
LD50 (mg/kg)		2160	-
Toxicity class		5	-
Organ Toxicity	**Hepatotoxicity**	Inactive	0.75
	Carcinogenicity	Inactive	0.63
	Immunotoxicity	Active	0.55
	Mutagenicity	Inactive	0.65
	Cytotoxicity	Inactive	0.79

Table 5. Pharmacological activities of the natural photosensitizer.

Properties	Propolis-benzofuran A	
	Pa	Pi
Membrane integrity agonist	0,846	0,025
HIF1A expression inhibitor	0,821	0,010
Hepatoprotectant	0,739	0,006
Chemopreventive	0,666	0,008
Membrane permeability inhibitor	0,645	0,064
Antiprotozoal (Leishmania)	0,639	0,012
Histidine kinase inhibitor	0,598	0,016
Anti-carcinogenic	0,549	0,015
Apoptosis agonist	0,547	0,033
Proliferative diseases treatment	0,520	0,017
Free radical scavenger	0,510	0,010
Anti-inflammatory	0,509	0,054
Antipruritic, allergic	0,434	0,067
Antiviral	0,422	0,070
Caspase 3 stimulant	0,402	0,050
Anti-mycobacterial	0,386	0,043
Anti-septic	0,242	0,054
Anti-mutagenic	0,230	0,065
Vasoprotector	0,282	0,184
Severe acute respiratory syndrome treatment	0,163	0,138